PNAS RESEARCH ARTICLE | APPLIED PHYSICAL SCIENCES BIOCHEMISTRY

Ultrafast spectra and kinetics of human green-cone visual pigment at room temperature

Dinesh Dhankhar[a], David Salom[b,c], Krzysztof Palczewski[b,c,d,e,f], and Peter M. Rentzepis[a,1]

Contributed by Peter M. Rentzepis; received August 30, 2022; accepted November 25, 2022; reviewed by Ali O. Er and Dmitri Voronine

Rhodopsin is the pigment that enables night vision, whereas cone opsins are the pigments responsible for color vision in bright-light conditions. Despite their importance for vision, cone opsins are poorly characterized at the molecular level compared to rhodopsin. Spectra and kinetics of the intermediate states of human green-cone visual pigment (mid-wavelength sensitive, or MWS opsin) were measured and compared with the intermediates and kinetics of bovine rhodopsin. All the major intermediates of the MWS opsin were recorded in the picosecond to millisecond time range. Several intermediates in MWS opsin appear to have characteristics similar to the intermediates of bovine rhodopsin; however, there are some marked differences. One of the most striking differences is in their kinetics, where the kinetics of the MWS opsin intermediates are slower compared to those of the bovine rhodopsin intermediates.

visual cycle | phototransduction | green cone-opsins | rhodopsin | 11-cis-retinal

Significance

Cone cells operate under photopic conditions (daytime, bright light, and color vision), which constitute a substantial portion of our vision. However, most of our understanding of the visual process comes from the study of rhodopsin, the visual pigment present in rod cells, which operates under dim light conditions. In this research, we conducted time-resolved (picoseconds to milliseconds) spectroscopic experiments and identified not only significant differences but also similarities in the light-induced photoproducts of the green-cone visual pigment versus rhodopsin.

Rods and cones are the light receptor cells present in the retinas of humans and other vertebrates. These two types of photoreceptor cells are responsible for vision under dim light conditions and color vision, respectively (1, 2). Rod cells operate in low light (scotopic vision) and are sufficiently sensitive to detect even a single photon (3–7). Three varieties of cone cells (blue, green, and red) in the human retina operate under brighter light, such as daylight (photopic vision) and together mediate the color vision (8).

Visual pigment proteins within the rod and cone cells detect light and initiate the process of vision (2). The visual pigments of these light-sensitive cells consist of an opsin protein coupled to a chromophore *via* a Schiff base linkage (9, 10). The visual pigment present in rod cells is rhodopsin, while the visual pigments present in the different types of cone cells are known as cone opsins. The nomenclature for cone opsins can be somewhat confusing. Ancestral vertebrates evolved four types of cone opsins: two short-wave-sensitive opsins (SWS1 and SWS2), a long- to middle-wave-sensitive opsin (LWS/MWS), and an additional middle-wave-sensitive (or rhodopsin-like opsin, RH2), initially called green-sensitive cone opsin. Additionally, these cone opsins can undergo multiple duplications or be lost in evolution; for example, due to their nocturnal adaptation, early mammals lost the SWS2 and RH2 opsins, whereas a duplication of the LWS/MWS opsin occurred in Old World monkeys 35 Mya. The combination of SWS1, MWS, and LWS cone opsins mediates trichromatic vision in humans and other apes (10).

For most vertebrates, the chromophore in the cone opsins and rhodopsin is the same, 11-*cis*-retinal. In the case of aquatic vertebrates, along with the 11-*cis*-retinal, they may have another, very similar chromophore 11-*cis*-didehydroretinal, with an extra double bond, as adaptation to changing habitat illumination (11–15).

Despite possessing the same 11-*cis*-retinal chromophore, the spectral sensitivities of rhodopsin and the different cone opsins are very different (1, 9, 10, 16, 17). These differences are attributed, to a large extent, to the amino acid substitutions in the opsin proteins (17, 18) which provide differences in the molecular environment of the retinal moiety (19). It is estimated that the substitution of a single amino acid may cause a spectral shift in wavelength sensitivity as large as 60 nm (10, 16, 20).

Besides their differences in wavelength sensitivity, the rod and cone visual pigments undergo a different regeneration cycle (21). It has been determined previously that the cone visual pigments regenerate at a much faster rate than rhodopsin (8, 21–23). A third difference between rods and cones is their distribution in the retina. While cones are concentrated mostly in a relatively small region near the fovea, rods are concentrated to a large extent in the peripheral region of the retina in the eyes of humans and other primates (1). Rods outnumber cones by a factor of 20:1 in human and other primates.

Genetically, it is estimated that opsins evolved from a single ancestral gene > 700 Mya (24), whereas rhodopsin started to diverge from RH2 cone opsin about 500 Mya (25). The amino acid sequence identity among human blue, green, and red cone opsins and rhodopsin in humans is around 40%, whereas red and green cone opsins display 96% identity (16).

Author affiliations: [a]Department of Electrical and Computer Engineering, Texas A&M University, College Station, TX 77843; [b]Department of Ophthalmology, Gavin Herbert Eye Institute, University of California Irvine, Irvine, CA 92697; [c]School of Medicine, University of California Irvine, Irvine, CA 92697; [d]Department of Chemistry, University of California Irvine, Irvine, CA 92697; [e]Department of Physiology and Biophysics, University of California Irvine, Irvine, CA 92697; and [f]Department of Molecular Biology and Biochemistry, University of California Irvine, Irvine, CA 92697

Author contributions: D.D. and P.M.R. designed research; D.D. performed research; D.S. and K.P. contributed new reagents/analytic tools; D.D. and P.M.R. analyzed data; and D.D. and P.M.R. wrote the paper.

Reviewers: A.O.E., Western Kentucky Universty; and D.V., University of South Florida.

The authors declare no competing interest.

[1]To whom correspondence may be addressed. Email: prentzepis@tamu.edu.

Published December 28, 2022.

We know much more about the light-induced molecular mechanisms of rhodopsin activation compared to cone opsins because rhodopsin kinetics and intermediates have been studied extensively since the 1950s; first at low temperatures and later at room temperature with the advent of lasers and time-resolved spectroscopic techniques (26–41). However, there have been few comparable experiments with the cone visual pigments (42–45). A vast majority of research on cone visual pigments has been conducted through electrophysiological/electroretinographic studies, or by means of time-resolved monitoring of the later intermediates in the photobleaching process (43, 44, 46–51). These indirect approaches have likely been prompted by the difficulties in purification and comparatively low stability of isolated cone visual pigments, resulting in only low yields of pure material (8, 52, 53). However, it is possible to produce cone visual pigments using recombinant techniques (54); recently, stable recombinant green-cone visual pigments were expressed at reasonable levels in insect *Sf9* cells and purified (53). We have utilized such recombinant human green-cone visual pigments for the time-resolved experiments presented here.

Our goal for the experiments described in this report were to determine and understand the kinetics of the human green-cone opsin visual pigments at room temperature, to answer questions concerning the kinetics of the initial intermediate in cone visual pigments and to determine how the results would compare with those for the rod visual pigment, rhodopsin. To these ends, we monitored the kinetics from the decay of the Batho-intermediate to the formation of the Meta-II intermediate and found the kinetics of the green-cone visual pigment to be slow in comparison to the kinetics of the rod visual pigment.

Results

Formation of Batho-Intermediate. After pumping the samples with a single picosecond light pulse, at 532 nm, a new red-shifted intermediate was observed almost immediately for the green-cone visual pigment as well as for the bovine rhodopsin (Fig. 1). The difference absorption (Δ OD) spectra displayed in Fig. 1*A* show a new red-shifted band with peak around 620 nm at 67 ps after excitation, when we used green-cone visual opsin. We assigned this new band to the Batho-intermediate of the green-cone visual opsin, corresponding to the Batho-rhodopsin formed in rhodopsin. After a 2-ns delay time, the 620-nm band blue-shifted slightly to about 610 nm.

The corresponding Δ OD spectra of bovine rhodopsin are shown in Fig. 1*B*. The Batho-rhodopsin intermediate in bovine rhodopsin showed a maximum at about 570 nm in the Δ OD spectra at 67 ps, and this band remained unchanged at 2 ns.

Decay of Batho-Intermediate and Formation of Lumi-Intermediate

After a further time delay of several nanoseconds, the new red-shifted intermediate of the human green-cone visual pigment decayed gradually and formed another intermediate with a Δ OD maximum of around 470 nm. The spectra and kinetics of this process from 4 ns to 1,000 ns are shown in Fig. 2 *A* and *B*, respectively.

Fig. 2*A* shows, clearly, that the red-shifted difference absorption (Δ OD) band decreases and converts into another intermediate whose Δ OD maximum is around 470 nm. There is an isosbestic point for this interconversion around 550 nm.

The kinetics of the decay at 610 nm and formation at 470 nm are well fitted by a single exponential relationship (Fig. 2*B*). The time constant for the decay at 610 nm was 243 ± 24 ns and 233 ± 28 ns for the formation at 470 nm, consistent with a single transition.

The difference spectra and kinetics of the intermediates of bovine rhodopsin are shown in Fig. 3 *A* and *B*, respectively. The decay at 570 nm corresponding to Batho-rhodopsin and the rise at 470 nm corresponding to the formation of Lumi-rhodopsin both show good fits to single exponential relationship with a time constant of 161 ± 14 ns for the Batho-rhodopsin decay and 192 ± 18 ns for the Lumi-rhodopsin formation (Fig. 3*B*).

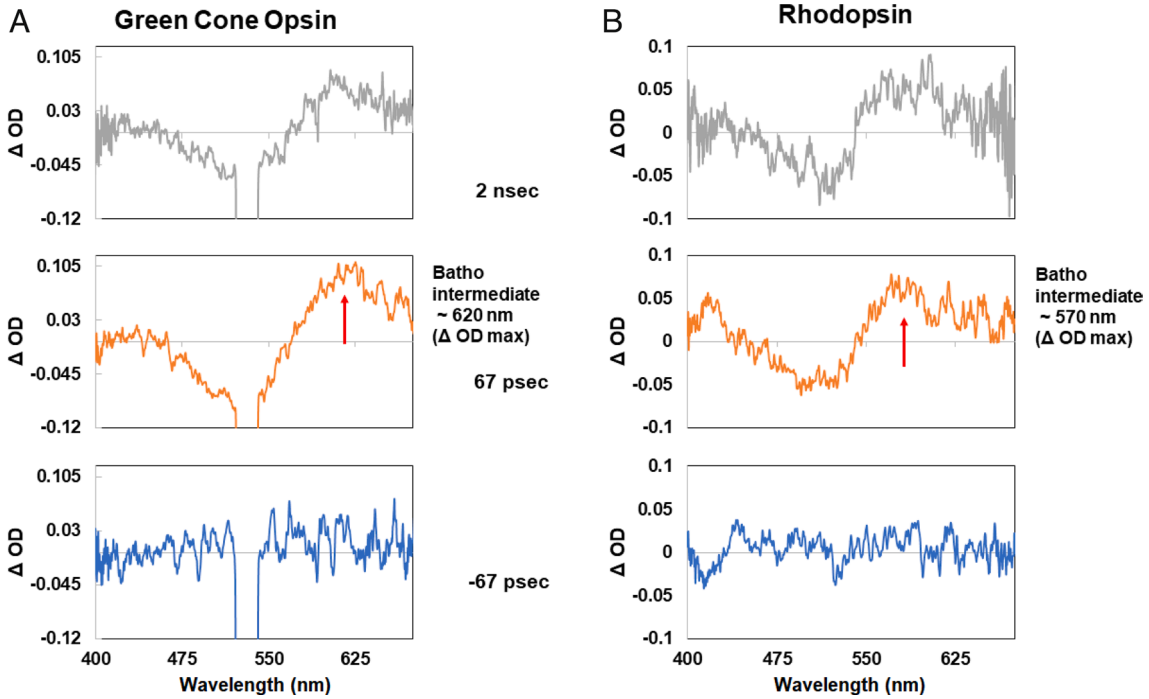

Fig. 1. Picosecond time-resolved spectra of the Batho-intermediates of the green-cone visual pigment (*A*) and bovine rhodopsin (*B*).

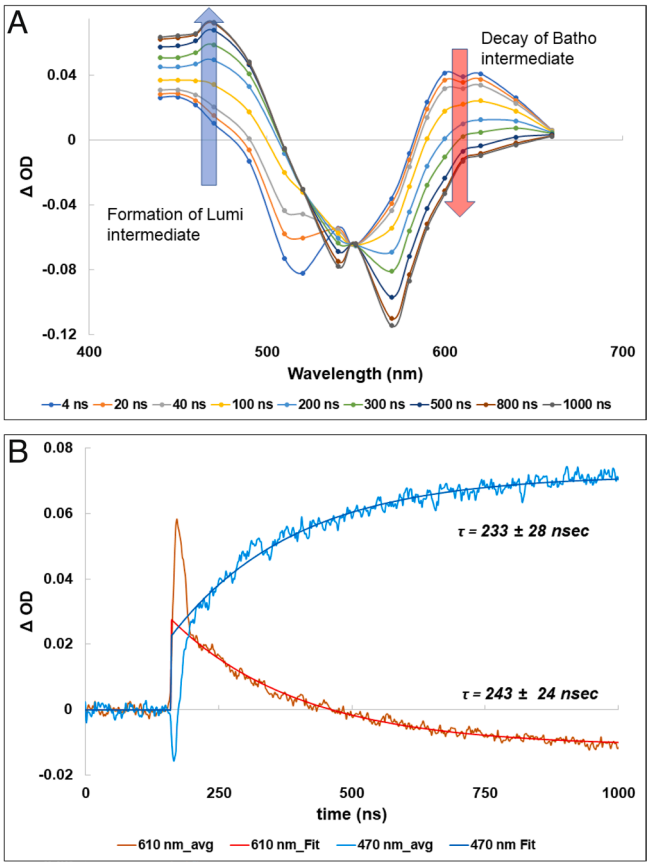

Fig. 2. Transient absorption spectra (*A*) and time course (*B*) of the decay of the Batho-intermediate at 610 nm and formation of the Lumi-intermediate of the green-cone visual pigment at 470 nm.

These data show that the kinetics of decay of the Batho/BL-intermediate and formation of the Lumi-intermediate for the green-cone visual pigment are slower than the corresponding transition process for bovine rhodopsin.

Lumi-Intermediate Decay and Meta-I Formation. Fig. 4*A* shows the Δ OD spectra from delay times of microseconds to 1 ms, after optical pumping with a nanosecond optical pulse of the green-cone visual pigment at 532 nm. The Lumi-intermediate was converted into another intermediate which has a slightly blue-shifted maxima (~10 to 12 nm) in the Δ OD spectrum. The isosbestic point for this conversion was around 476 nm (Fig. 4*A*). The time constant for this conversion was measured to be ~47 μs (Fig. 4*C*). We identify this intermediate to be equivalent to the Meta-I intermediate of bovine rhodopsin.

Meta-I Decay and Meta-II Formation. The Meta-I intermediate decays and forms another new intermediate, which we identify as the Meta-II intermediate, with a Δ OD maximum near 385 nm (Fig. 4*B*). Fig. 4 *B* and *D* shows the transient absorption spectra and kinetics, respectively, of the Meta-I to Meta-II conversion for the green-cone visual pigment. The isosbestic point for this conversion was ~420 nm (Fig. 4*B*) and the time constant for Meta-II formation was 5 to 6 ms (Fig. 4*D*).

Comparison of the kinetics for Meta-I and Meta-II formation for human green-cone opsin versus bovine rhodopsin shows that the green-cone opsins are slower. The time constants for the formation of Meta-I were ~47 μs for green-cone opsin (this study) and ~10 μs for bovine rhodopsin (55). Similarly, the measured time constants for Meta-II formation were ~6 ms (green-cone opsin) and ~1.5 ms (bovine rhodopsin).

In addition to the lifetime differences of the opsin-intermediates in rods and cones, the shape of the difference absorption spectrum for the formation of the Meta-II intermediate of the green-cone visual pigment appears different from that for bovine rhodopsin (Fig. 5). We interpret this difference, in shape, to reflect that for the green-cone visual pigment, the Meta-I intermediate is not fully converted into Meta-II, but rather exists in dynamic equilibrium state where some of the Meta-II is converted back to Meta-I.

Discussion

This is the direct characterization of the kinetics of light-induced transitions in human cone visual pigments. Our data show interesting similarities and differences between the green-cone visual pigment and rhodopsin.

The similarities in their mechanism of response to light include very fast [less than the experimental time resolution of 28 ps and probably within femtoseconds (34)] formation of the first spectral intermediate, Batho, with a red-shifted absorption band at room temperature and gradual transition to later intermediates that show spectral shifts of the absorption maxima toward shorter and shorter wavelengths. The final intermediates for both the human green-cone visual pigment and the bovine rod visual pigment were found to have an absorption maximum near 380 nm.

However, a closer look at each individual intermediate shows that there are several spectral and kinetic differences between the responses of the green-cone visual pigment and the rod visual pigment. The difference spectrum reflecting the formation of the Batho-intermediate shows a shift of about 90 nm (530 nm to 620 nm) for the green-cone visual pigment, however a shift of about 70

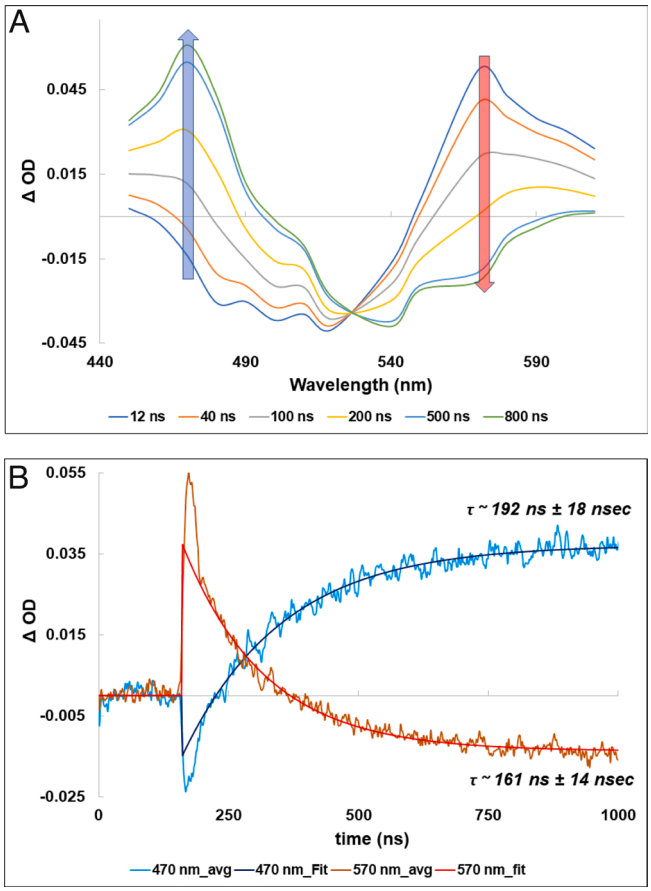

Fig. 3. Transient absorption spectra (*A*) and time course (*B*) of the decay of the Batho-intermediate at 570 nm and formation of the Lumi-intermediate of bovine rhodopsin at 470 nm.

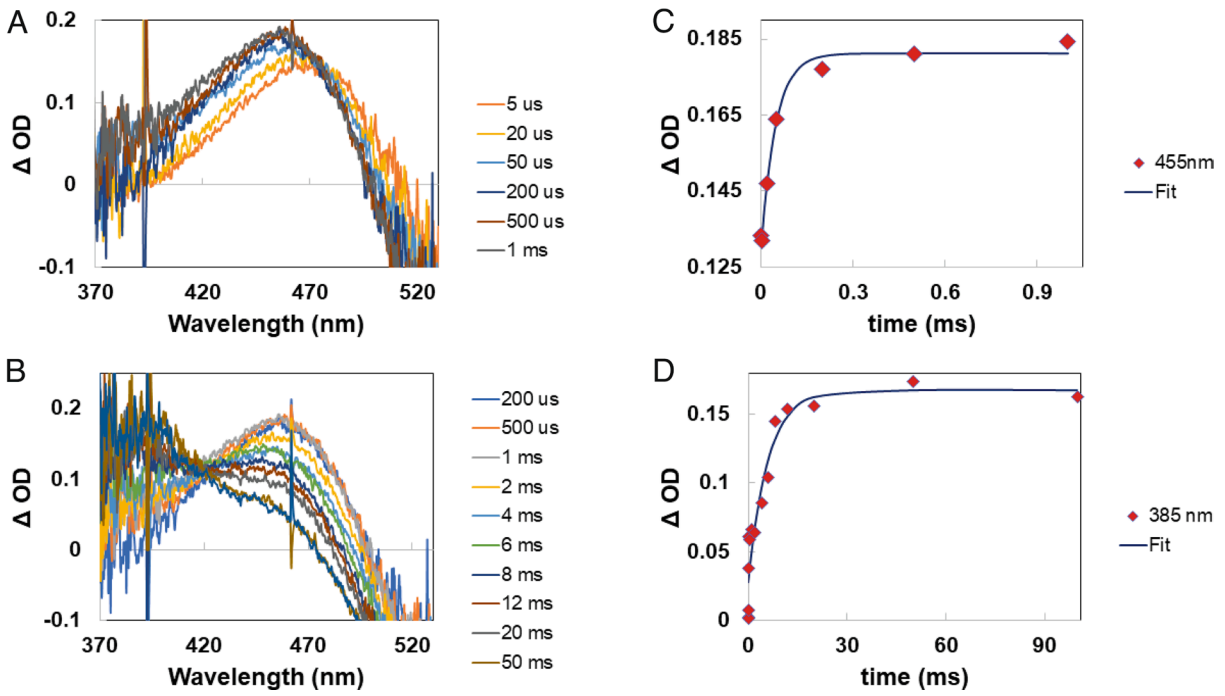

Fig. 4. Microsecond to millisecond spectral changes and kinetics for green-cone opsins. (*A*) Lumi to Meta-I intermediate conversion with green-cone opsins. (*B*) Decay of Meta-I intermediate and formation of Meta-II intermediate of green-cone opsin. (*C*) Lumi to Meta-I conversion kinetics measured at 455 nm, and (*D*) Meta-I to Meta-II intermediate conversion kinetics at 385 nm.

nm (500 nm to 570 nm) for the bovine rod visual pigment. In addition, the Batho-intermediate of the rod visual pigment decays straightforwardly to the Lumi-intermediate, whereas the conversion of the Batho-intermediate of the green-cone visual pigment to its Lumi-intermediate appears to be more complicated, involving another transient intermediate between the Batho- and Lumi-intermediates. This interpretation is based on the small shift in the Δ OD spectrum for the green-cone visual pigment which occurs between 67 ps and 2 ns, suggesting that the Batho-intermediate first decays to another intermediate within a few nanoseconds and this intermediate is the precursor to the Lumi-intermediate, with a time constant of about 240 ns. We could name this post-Batho-intermediate of the green-cone visual pigment as the "BL intermediate" by analogy to the report of Shichida et al. (56), where such an intermediate was observed with the chicken red-cone visual pigment.

The differences in the Batho-intermediate spectra, observed in bovine rhodopsin and green-cone opsin, are attributed to the differences in their protein structure.

Our studies also document differences in the kinetics of interconversion between the various intermediates for the green-cone visual pigment versus the rod visual pigment. For example, the time constants for transition to the Lumi-intermediate were about 40% larger for the human green-cone visual pigment versus bovine rhodopsin (Fig. 6). We attribute these differences in the decay and formation lifetimes to the differences in the structures of the green-cone visual pigment and bovine rod visual pigment. It would be interesting to see how the kinetics change among the different cone visual pigments such as red, green, and blue visual pigments.

This difference in kinetics is more striking for the Lumi to Meta-I transition, where the time constant for the green-cone visual

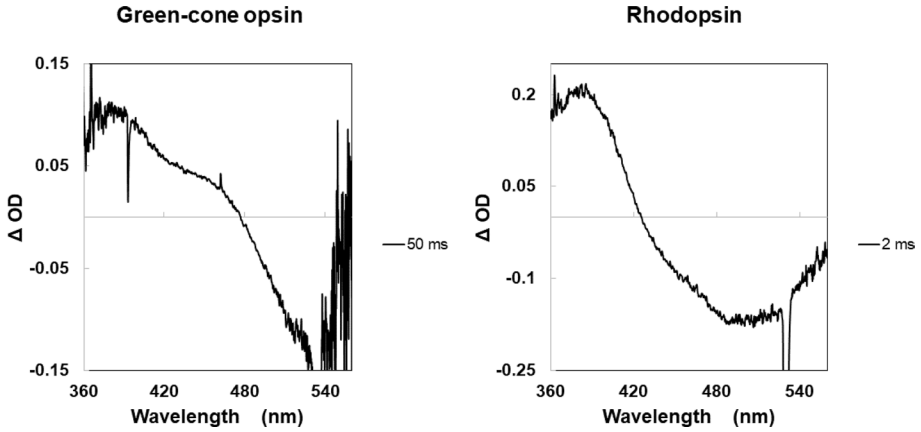

Fig. 5. Comparison of typical Δ OD spectra of green-cone opsin and bovine rhodopsin for formation of Meta-II. The difference in their shapes is attributed to incomplete conversion of the Meta-I to the Meta-II intermediate with green-cone opsin, suggesting considerable reversal of Meta-II to Meta-I.

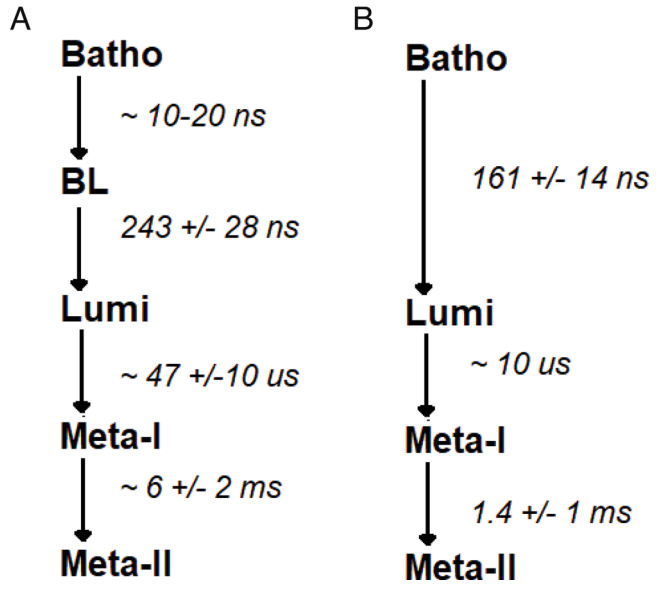

Fig. 6. Comparison of the major photointermediates of human green-cone (*A*) and bovine rod (*B*) visual pigments.

pigment was found to be 5 times larger than that reported for the rod visual pigments (55). For the Meta-I to Meta-II transition, not only are the kinetics different (~4X slower for green-cone visual pigment versus rhodopsin), but also the nature of the interconversion appears to be different. For bovine rod visual pigment, there is essentially complete conversion of Meta-I to Meta-II, whereas there appears to be only a partial conversion for human green-cone visual pigment. This incomplete transition suggests a dynamic interconversion between Meta-I and Meta-II forms of the green-cone visual pigment. This behavior was also seen earlier in the chicken red cone studies (56); however, the effect is more prominent in the present study. One possible reason for the incomplete conversion could be artificially related to the protein construct used in this study. For example, the fusion protein inserted into the third intracellular loop (see *Methods*) might restrict the conformational changes required to adopt the Meta-II conformation.

Even though the photobleaching of intermediates in green cones is found to be slower compared to rods, the regeneration of the visual pigment in a solution of opsin and chromophore (11-*cis*-retinal) proceeds much faster in cones (a few minutes) as compared to rods (a few hours), a difference of more than 100 times in the regeneration rate (22, 23, 56). As far as the effect of detergent medium on the kinetics is concerned, it has been shown that the properties of detergent medium can influence the kinetics of Meta intermediates, whereas Batho- and Lumi–intermediates' kinetics are virtually unaffected by it (57).

It would be interesting to observe, also, similar kinetics for red and blue cones. For the red cones, we expect similar kinetics because not only the green and red cones are close in their spectral absorption, but also they are very close in their amino acid sequence (10, 17). Blue cones, on the contrary, are much more distinct from rod and rest of the cones (10, 17) in their genetic evolution, amino acid sequence, and spectral response, which may result in different kinetics or intermediates in blue cones. We are currently in the process of obtaining samples for a similar study on blue cone opsin kinetics.

Conclusion

The kinetics and spectra of light-induced intermediates of human green-cone visual pigment, recorded (at picoseconds to hundreds of milliseconds) after laser pulse excitation, were compared with those of bovine rhodopsin. The basic sequence of formation and spectral nature of the intermediates were found to be very similar for the two types of visual pigments. However, the decay and formation kinetics for most of the intermediates of the human green-cone visual pigments were slower than those for the bovine rod visual pigment. In addition, there appears to be another intermediate between the Batho- and Lumi-intermediates of the human green-cone visual pigment. The possible biological significance of the differences in the kinetics between rods and cones could give a better understanding of color vision in humans and other animals.

Materials and Methods

Time-Resolved Absorption System, Nanoseconds to Milliseconds. Our experimental system has been described previously (55). Briefly, the second harmonic of a Q-switched, 8 ns pulse width, Nd:YAG laser (Newwave Research, Model Tempest 213), at 532 nm, was utilized to optically pump the rod and cone opsin samples. A longer duration flashlamp (FWHM ~100 μs) whose peak flash intensity was synchronized with the pumping laser pulse was utilized as the probe source. The changes in intensity of the flash probe induced by the optical pumping were monitored by a photomultiplier tube (PMT, RCA 928) attached to the exit slit of a Jarrell Ash Model 82-410 monochromator. The kinetic data at various wavelengths were recorded with a fast sampling oscilloscope (Tektronix, TDS3052B, 5 Giga Samples per second, 0.5 GHz Bandwidth), with 50 Ohm input impedance. The 532-nm pump laser's pulse width was ~8 ns and its energy 200 mJ per pulse.

The same system has a provision for a second flashlamp probe (200 ns FWHM pulse width), where the probe flash can be electronically delayed with respect to the excitation pump laser pulse. Changes in the spectra and intensity of the probe light transmitted through the sample were monitored by means of a CCD spectrometer (B&W Tek) as a function of the delay with respect to the pump pulse. With the combination of these two systems, the spectra and kinetics of the visual pigments were determined from nanoseconds to seconds after excitation. Fig. 7 shows a schematic diagram of a nanosecond experimental system.

Picosecond Time-Resolved Absorption System. This experimental system allows us to record the time-resolved absorption spectra from 28 ps to 4 ns. The system consists of a picosecond laser (Ekspla, PL2230), with a pulse width of 28 ps (30 mJ energy) at 1,064 nm. A portion of the energy, in the primary beam, was passed through a H_2O:D_2O mixture in order to generate a white light continuum, which we used to probe. Another portion of the energy was converted to 532 nm, using a second harmonic generator crystal (Fig. 2); the energy of the 532-nm pump pulse was ~10 mJ. The probe pulse was delayed with respect to the pump pulse by means of a delay stage. A spectrometer (Acton Research Corporation Model: SpectraPro 150) with a cooled CCD camera (Princeton Instruments PIXIS 400) was used to record the spectra at different pump–probe delay times. Fig. 8 shows a schematic diagram of our experimental system used for the picosecond time-resolved absorption spectroscopy.

Preparation of Samples of Human Green-Cone Visual Pigment and Bovine Rhodopsin. Human green-cone opsin and bovine rhodopsin were purified by immunochromatography under dim red light (> 670 nm). Human green-cone opsin was generated recombinantly in Sf9 insect cells and purified according to the procedure described in (53); a brief description is presented here. The DNA construct for green-cone opsin was synthesized by GenScript (Piscataway, NJ). The corresponding protein consisted of human MWS opsin sequence in which the C terminus was truncated at residue 343 and replaced with anti-rhodopsin 1D4 antibody epitope TETSQVAPA, and the third intracellular loop (residues 251 to 257) was replaced by a modified T4 lysozyme (UNIPROT ID P00720, with M^1 and its three C-terminal residues truncated, and mutations C54T and C97A).

Bacmid was produced using the Bac-to-Bac Baculovirus Expression System Protocol by Invitrogen (Carlsbad, CA). Initial transfection was achieved by adding 1 μg of bacmid DNA to log phase *Sf9* cells. The supernatant was harvested after 5 d and P1 virus was added to 40 mL of cells (1.5×10^6 cells/mL). After 4 d, the P2 virus was harvested by centrifuging the culture at 2,500 g for 5 min. P3 virus stock was prepared by adding 2 mL of P2 virus to 800 mL of Sf9 cells (2×10^6

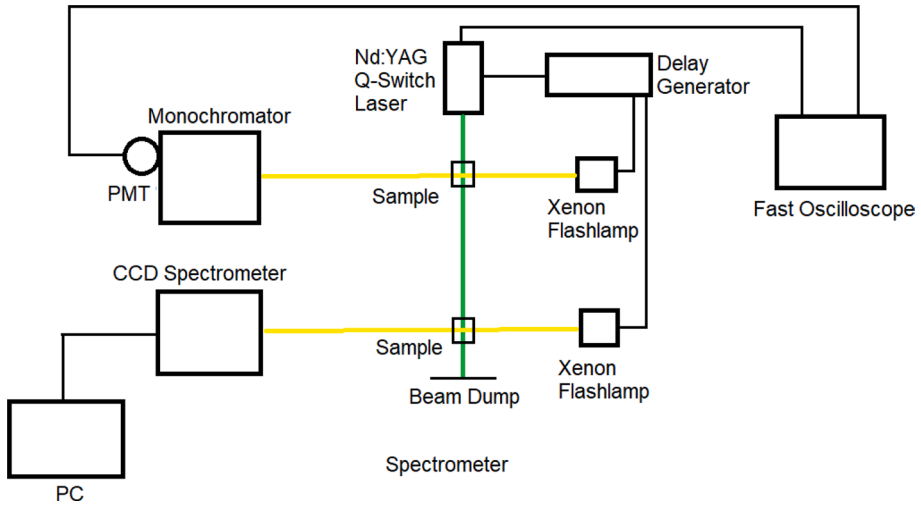

Fig. 7. Schematic diagram of the nanosecond to seconds time-resolved absorption spectroscopy system.

cells/mL). After 3 d, P3 virus was harvested in a similar manner as P2 virus and used to optimize the expression.

Frozen Sf9 cells were thawed in a hypotonic buffer (10 mM HEPES pH 7.4, 1 mM $MgCl_2$ containing DNase and protease inhibitors) and disrupted in a Dounce homogenizer. Membranes were pelleted by centrifugation at 50,000 g for 50 min and homogenized/ centrifuged again in the hypotonic buffer. Subsequently, the homogenization and centrifugation were repeated 2 to 3 times in the same buffer containing 1 M NaCl. The washed membranes were resuspended in 50 mM HEPES pH 7.4, 0.15 M NaCl, and 30 μM 11-*cis*-retinal was added to reconstitute the green-cone opsin. After 30 min incubation on ice, the membranes were solubilized with lauryl maltose neopentyl glycol (LMNG) at a ratio of 50 mg of LMNG per gram of membrane. The suspension was mixed for 3 h and the insoluble material was removed by centrifugation at 50,000 g for 50 min. Green-cone opsin was purified from the supernatant by immunoaffinity chromatography with immobilized 1D4 antibody, and it was eluted with 1 mM TETSQVAPA peptide (53).

Rod outer segments (ROS) were enriched from dark-adapted frozen retinas with a step-sucrose gradient following established protocols (58). Bovine rhodopsin was purified by solubilizing ROS in LMNG and following the same immunochromatographic procedure described above for green-cone opsin tagged with the rhodopsin TETSQVAPA sequence at the C terminus.

UV–Vis spectra were recorded with a Cary 50 Bio UV-Vis spectrophotometer and a Shimadzu 1601 UV-Vis spectrophotometer. The absorption spectra of purified cones and rod opsin pigments are shown in Fig. 9. The proteins were concentrated with a 30-kDa centrifugal concentrator to reach a peak optical density of ~1 (1 cm path length) at 500 nm or 530 nm for bRho or MWS opsin, respectively.

For the time-resolved experiments, the samples were placed in a microchannel cuvette (10 to 15 μL) and were replaced with a fresh sample after each laser shot in order to avoid bleaching of the samples. Further, all the experiments were conducted in the dark, and sample replacement was carried out under dim red light to avoid any bleaching of the samples.

Data Analysis. For the picosecond experiments, the spectra at different pump–probe delay times were recorded by the spectrometer and CCD camera and converted to delta OD spectra using WinSpec software (Princeton Instruments).

For nanosecond to microsecond experiments, the recorded transient kinetic data recorded on the oscilloscope were converted to delta OD values at each wavelength. Subsequently, the kinetics at all wavelengths were fitted to a single

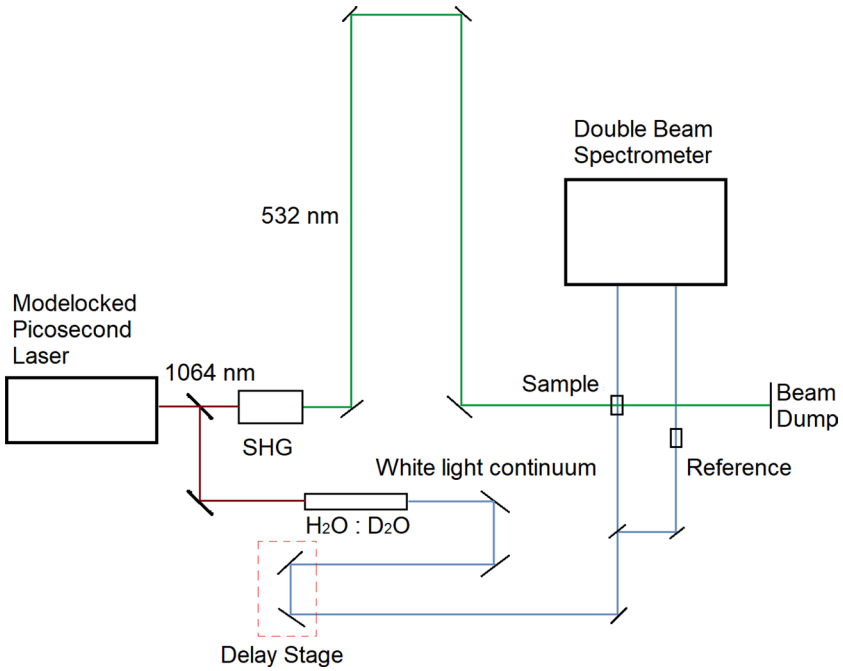

Fig. 8. Schematic of the picosecond time-resolved absorption setup.

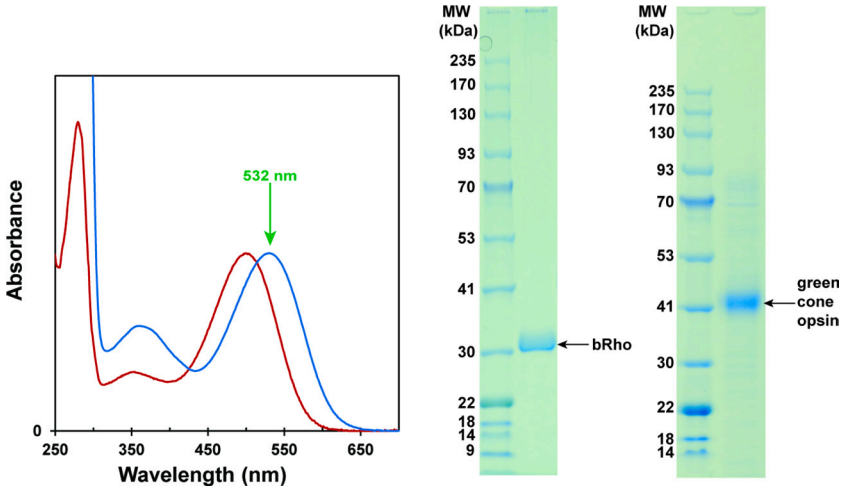

Fig. 9. Normalized absorption spectra of purified fractions of bovine rhodopsin (red) and green-cone opsin (blue) to be used in the experiments. Green arrow shows the pump wavelength. On the right are shown the purification gel results for bovine rhodopsin (bRho) and green-cone opsin.

exponential decay (from 40 ns to 1,000 ns) using ImageJ software. The transient absorption spectra were derived from these fits, for nanosecond to microsecond time delays. For the microsecond to millisecond time delays, the spectra were recorded directly at different time delays using the spectrometer.

Data, Materials, and Software Availability. All study data are included in the main text.

ACKNOWLEDGMENTS.. We thank Arjun Krishnamoorthi for technical assistance during the experiments. This study was supported by Air Force Office of Scientific Research (AFOSR) Grant #FA9550-20-1-0139 and by Texas A&M Engineering Experiment Station (TEES) funds. This research was supported in part also by NIH research grant EY030873 (NEI) to K.P.; we also acknowledge support from a Research to Prevent Blindness Unrestricted Grant to the Department of Ophthalmology at University of California, Irvine.

1. D. Mustafi, A. H. Engel, K. Palczewski, Structure of cone photoreceptors. *Prog. Retin. Eye Res.* **28**, 289–302 (2009).
2. V. J. Kefalov, Rod and cone visual pigments and phototransduction through pharmacological, genetic, and physiological approaches. *J. Biol. Chem.* **287**, 1635–1641 (2012).
3. D. A. Baylor, T. D. Lamb, K. W. Yau, Responses of retinal rods to single photons. *J. Physiol.* **288**, 613–634 (1979).
4. F. Rieke, D. A. Baylor, Single-photon detection by rod cells of the retina. *Rev. Mod. Phys.* **70**, 1027–1036 (1998).
5. F. Rieke, "Mechanisms of single-photon detection in Rod photoreceptors" in *Methods in Enzymology*, K. Palczewski, Ed. (Vertebrate Phototransduction and the Visual Cycle, Part B, Academic Press, 2000), **vol. 316**, pp. 186–202.
6. J. Reingruber *et al.*, Detection of single photons by toad and mouse rods. *Proc. Natl. Acad. Sci. U.S.A.* **110**, 19378–19383 (2013).
7. K. Palczewski, G protein-coupled receptor rhodopsin. *Annu. Rev. Biochem.* **75**, 743–767 (2006).
8. Y. Imamoto, Y. Shichida, Cone visual pigments. *Biochim. Biophys. Acta* **1837**, 664–673 (2014).
9. S. Yokoyama, Molecular evolution of vertebrate visual pigments. *Prog. Retinal Eye Res.* **19**, 385–419 (2000).
10. J. K. Bowmaker, Evolution of vertebrate visual pigments. *Vision Res.* **48**, 2022–2041 (2008).
11. G. Wald, The porphyropsin visual system. *J. Gen. Physiol.* **22**, 775–794 (1939).
12. G. L. Fain, Phototransduction: Making the chromophore to see through the murk. *Curr. Biol.* **25**, R1126–R1127 (2015).
13. T. E. Reuter, R. H. White, G. Wald, Rhodopsin and porphyropsin fields in the adult bullfrog retina. *J. Gen. Physiol.* **58**, 351–371 (1971).
14. S. M. Mohun, W. I. L. Davies, The evolution of amphibian photoreception. *Front. Ecol. Evol.* **7**, 1–12 (2019).
15. J. C. Corbo, Vitamin A(1)/A(2) chromophore exchange: Its role in spectral tuning and visual plasticity. *Dev. Biol.* **475**, 145–155 (2021).
16. J. Nathans, D. Thomas, D. S. Hogness, Molecular genetics of human color vision: The genes encoding blue, green, and red pigments. *Science* **232**, 193–202 (1986).
17. S. Yokoyama, Molecular evolution of vertebrate visual pigments. *Prog. Retin. Eye Res.* **19**, 385–419 (2000).
18. H. Imai *et al.*, Single amino acid residue as a functional determinant of rod and cone visual pigments. *Proc. Natl. Acad. Sci. U.S.A.* **94**, 2322–2326 (1997).
19. T. P. Sakmar, Redder than red. *Science* **338**, 1299–1300 (2012).
20. S. E. Wilkie *et al.*, Spectral tuning of avian violet- and ultraviolet-sensitive visual pigments. *Biochemistry* **39**, 7895–7901 (2000).
21. J. S. Wang, V. J. Kefalov, The cone-specific visual cycle. *Prog. Retin. Eye Res.* **30**, 115–128 (2011).
22. G. Wald, P. K. Brown, P. H. Smith, Iodopsin. *J. Gen. Physiol.* **38**, 623–681 (1955).
23. Y. Shichida, H. Imai, Y. Imamoto, Y. Fukada, T. Yoshizawa, Is chicken green-sensitive cone visual pigment a rhodopsin-like pigment? A comparative study of the molecular properties between chicken green and rhodopsin. *Biochemistry* **33**, 9040–9044 (1994).
24. R. Feuda, S. C. Hamilton, J. O. McInerney, D. Pisani, Metazoan opsin evolution reveals a simple route to animal vision. *Proc. Natl. Acad. Sci. U.S.A.* **109**, 18868–18872 (2012).
25. T. Baden, D. Osorio, The retinal basis of vertebrate color vision. *Annu. Rev. Vis. Sci.* **5**, 177–200 (2019).
26. T. Yoshizawa, G. Wald, Pre-lumirhodopsin and the bleaching of Visual Pigments. *Nature* **197**, 1279–1286 (1963).
27. P. K. Brown, G. Wald, Visual pigments in single rods and cones of the human retina. *Science* **144**, 45–52 (1964).
28. T. L. Netzel, P. M. Rentzepis, J. Leigh, Picosecond kinetics of reaction centers containing bacteriochlorophyll. *Science.* **182**, 238–241 (1973).
29. R. Bensasson, E. J. Land, T. G. Truscott, Nanosecond flash photolysis of rhodopsin. *Nature* **258**, 768–770 (1975).
30. D. Huppert, P. M. Rentzepis, G. Tollin, Picosecond kinetics of chlorophyll and chlorophyll/quinone solutions in ethanol. *Biochim. Biophys. Acta.* **440**, 356–364 (1976).
31. P. M. Rentzepis, "Picosecond spectroscopy in biological systems" in *Methods in Enzymology*, S. Fleischer, L. Packer, Eds. (Biomembranes - Part E: Biological Oxidations, Academic Press, 1978), **vol. 54**, pp. 3–32.
32. J. S. Horwitz, J. W. Lewis, M. A. Powers, D. S. Kliger, Nanosecond laser photolysis of rhodopsin and isorhodopsin. *Photochem. Photobiol.* **37**, 181–188 (1983).
33. Y. G. Thomas, I. Szundi, J. W. Lewis, D. S. Kliger, Microsecond time-resolved circular dichroism of rhodopsin photointermediates. *Biochemistry* **48**, 12283–12289 (2009).
34. O. A. Smitienko *et al.*, Femtosecond formation dynamics of primary photoproducts of visual pigment rhodopsin. *Biochemistry (Mosc).* **75**, 25–35 (2010).
35. O. P. Ernst *et al.*, Microbial and animal rhodopsins: Structures, functions, and molecular mechanisms. *Chem. Rev.* **114**, 126–163 (2014).
36. M. N. Sandberg *et al.*, Low-temperature trapping of photointermediates of the rhodopsin E181Q mutant. *SOJ Biochem.* **1**, 1–12 (2014).
37. T. B. Feldman *et al.*, Femtosecond spectroscopic study of photochromic reactions of bacteriorhodopsin and visual rhodopsin. *J. Photochem. Photobiol. B: Biol.* **164**, 296–305 (2016).
38. M. Olchawa *et al.*, In vitro phototoxicity of rhodopsin photobleaching products in the retinal pigment epithelium (RPE). *Free Radic. Res.* **53**, 456–471 (2019).
39. S. Tahara, H. Kuramochi, S. Takeuchi, T. Tahara, Protein dynamics preceding photoisomerization of the retinal chromophore in bacteriorhodopsin revealed by deep-UV femtosecond stimulated raman spectroscopy. *J. Phys. Chem. Lett.* **10**, 5422–5427 (2019).
40. M. A. Ostrovsky, V. A. Nadtochenko, Femtochemistry of rhodopsins. *Russ. J. Phys. Chem. B.* **15**, 344–351 (2021).
41. J.-H. Yun *et al.*, Early-stage dynamics of chloride ion–pumping rhodopsin revealed by a femtosecond X-ray laser. *Proc. Natl. Acad. Sci. U.S.A.* **118**, e2020486118 (2021).
42. H. Kandori *et al.*, Bathoiodopsin, a primary intermediate of iodopsin at physiological temperature. *Proc. Natl. Acad. Sci. U.S.A.* **87**, 8908–8912 (1990).
43. V. L. Mooney, I. Szundi, J. W. Lewis, E. C. Y. Yan, D. S. Kliger, Schiff base protonation changes in Siberian hamster ultraviolet cone pigment photointermediates. *Biochemistry* **51**, 2630–2637 (2012).
44. K. Sato, T. Yamashita, Y. Imamoto, Y. Shichida, Comparative studies on the late bleaching processes of four kinds of cone visual pigments and rod visual pigment. *Biochemistry* **51**, 4300–4308 (2012).
45. J. Liang, R. Govindjee, T. G. Ebrey, Metarhodopsin intermediates of the gecko cone pigment P521. *Biochemistry* **32**, 14187–14193 (1993).
46. M. H. Howlett, R. G. Smith, M. Kamermans, A novel mechanism of cone photoreceptor adaptation. *PLoS Biol.* **15**, e2001210 (2017).
47. R. Sinha *et al.*, Cellular and circuit mechanisms shaping the perceptual properties of the primate Fovea. *Cell* **168**, 413–426.e12 (2017).

48. J. Baudin, J. M. Angueyra, R. Sinha, F. Rieke, S-cone photoreceptors in the primate retina are functionally distinct from L and M cones. *Elife.* **8**, e39166 (2019).
49. M. H. Berry *et al.*, Restoration of high-sensitivity and adapting vision with a cone opsin. *Nat. Commun.* **10**, 1221 (2019).
50. Y. Cao *et al.*, Interplay between cell-adhesion molecules governs synaptic wiring of cone photoreceptors. *Proc. Natl. Acad. Sci. U.S.A.* **117**, 23914–23924 (2020).
51. Y. Imamoto, I. Seki, T. Yamashita, Y. Shichida, Efficiencies of activation of transducin by cone and rod visual pigments. *Biochemistry* **52**, 3010–3018 (2013).
52. R. Hubbard, The thermal stability of rhodopsin and opsin. *J. Gen. Physiol.* **42**, 259–280 (1958).
53. T. S. Owen, D. Salom, W. Sun, K. Palczewski, Increasing the stability of recombinant human green cone pigment. *Biochemistry* **57**, 1022–1030 (2018).
54. P. M. Vissers, P. H. Bovee-Geurts, M. D. Portier, C. H. Klaassen, W. J. Degrip, Large-scale production and purification of the human green cone pigment: Characterization of late photo-intermediates. *Biochem. J.* **330**, 1201–1208 (1998).
55. D. Dhankhar *et al.*, Comparison of bovine and carp fish visual pigment photo-intermediates at room temperature. *Photochem. Photobiol.* **98**, 1303–1311 (2022), 10.1111/php.13621.
56. Y. Shichida, T. Okada, H. Kandori, Y. Fukada, T. Yoshizawa, Nanosecond laser photolysis of iodopsin, a chicken red-sensitive cone visual pigment. *Biochemistry* **32**, 10832–10838 (1993).
57. J. Epps, J. W. Lewis, I. Szundi, D. S. Kliger, Lumi I → Lumi II: The last detergent independent process in rhodopsin photoexcitation. *Photochem. Photobiol.* **82**, 1436–1441 (2006).
58. D. S. Papermaster, Preparation of retinal rod outer segments. *Methods Enzymol.* **81**, 48–52 (1982).